

# Step-edge instability during epitaxial growth of graphene from SiC(0001)

Valery Borovikov\* and Andrew Zangwill†

*School of Physics, Georgia Institute of Technology, Atlanta, Georgia 30332, USA*

(Received 10 August 2009; published 25 September 2009)

A continuum equation for step motion is used to explain fingerlike structures observed when graphene is grown epitaxially by step flow decomposition of SiC(0001). A linear stability analysis predicts when a morphological perturbation of a straight moving step grows or decays as a function of growth temperature, the background pressure of Si maintained during growth, and the presence of an inert buffer gas used to retard the escape of Si atoms from the crystal surface. The theory gives semiquantitative agreement with experiment for the characteristic separation between fingers observed when graphene is grown in a low-pressure induction furnace or under ultrahigh vacuum conditions. A local heating mechanism is proposed as the driving force for instability.

DOI: [10.1103/PhysRevB.80.121406](https://doi.org/10.1103/PhysRevB.80.121406)

PACS number(s): 68.55.A–, 61.46.–w, 81.10.Aj

The unique electronic properties of graphene offer the possibility that it could replace silicon when microelectronics evolves to nanoelectronics.<sup>1</sup> Graphene grown epitaxially on silicon carbide<sup>2</sup> is particularly attractive for future nanoelectronics because SiC is itself a useful semiconductor and, by suitable manipulation of the growth conditions,<sup>3–5</sup> epitaxial films can be produced that exhibit all the transport properties of ideal, two-dimensional graphene desired for device applications.<sup>6–8</sup> Nevertheless, there is little or no understanding of the actual kinetics of growth, which is likely to be required for future process control. Our focus here is a fingerlike pattern observed for the shape of steps when graphene is grown by step flow decomposition of the silicon-terminated surface of SiC(0001). The problem is interesting because, if we accept the most likely growth scenario for this system,<sup>9</sup> it is very unlikely that the fingering arises from a Mullins-Sekerka instability that arises when the transport of atomic species to and from steps is controlled by surface diffusion on the terraces and the attachment/detachment kinetics at a step is asymmetric.<sup>10,11</sup>

Figure 1 is an atomic force microscope image of 2–3 ML of graphene grown on a commercial wafer of SiC(0001) at  $\sim 1600^\circ\text{C}$  in a low-pressure induction furnace.<sup>12</sup> The original wafer was H-etched at high temperature to produce a regular array of steps.<sup>13,14</sup> When heated above the graphitization temperature,  $T_G$ , the steps bunch into macrosteps (which run vertically in Fig. 1) separated by large nearly flat terraces. A continuous and conformal film of graphene covers the entire sample. Nevertheless, a step with a highly ramified edge appears clearly between each pair of adjacent macrosteps. Very similar fingering has been reported when graphene films are grown in an argon atmosphere<sup>15</sup> and a highly ramified step morphology has also been reported for graphene grown on a vicinal surface of SiC(0001) under ultrahigh vacuum (UHV) conditions.<sup>16</sup> The thermal decomposition process that produces graphene occurs preferentially at steps, where Si and C atoms are least well bonded. Figure 2(a) shows a step on SiC(0001) covered conformally by one complete layer of graphene and a second incomplete layer.<sup>9</sup> The diagram reflects the fact that, above  $\sim 1100^\circ\text{C}$ , the bulk of the SiC crystal is “buffered” from anything that lies above (vacuum or graphene) by a carbon-rich  $6\sqrt{3} \times 6\sqrt{3}$  recon-

struction. The structure of the buffer layer is not completely known, but it apparently resembles graphene itself, albeit distorted so it bonds strongly to the silicon layer immediately below.<sup>17</sup> When the temperature exceeds  $1200^\circ\text{C}$ , the SiC beneath the buffer layer of the upper terrace begins to decompose. The liberated Si atoms desorb, the upper buffer layer transforms to graphene, and the liberated C atoms recrystallize at the base of the step to extend the lower buffer layer. Figure 2(b) shows the advance of the second graphene layer. The growth scenario sketched above requires very little motion of the carbon atoms. Silicon atom diffusion is important, but the transport of atoms *away* from a step does not lead to morphological instability.<sup>18</sup> Therefore, despite their appearance, the fingers in Fig. 1 probably do not arise from a Mullins-Sekerka-type morphological instability.<sup>10,11</sup> This leads us to offer primarily a phenomenological analysis and only at the end do we propose a possible microscopic mechanism for the instability.

The quantity of interest is the position  $h(x, t)$  of a SiC step edge, for which we seek a continuum equation of motion. The key assumption is that the decomposition of a SiC step edge depends on the local curvature of the front; a higher rate for concave regions and a lower rate for convex regions. If true, Fig. 3 shows how the step edge between graphene and the upper buffer layer may be expected to evolve as time goes on. Comparison with Fig. 1 identifies the light-colored fingers as buffer layer and the darker channels between them as graphene. If  $V$  is the average velocity of the step due to decomposition, a suitable evolution equation for  $h(x, t)$  is

$$\frac{\partial h}{\partial t} = -V - aV \frac{\partial^2 h}{\partial x^2} + \sigma \Gamma \frac{\partial^2 h}{\partial x^2} - \sigma D \frac{\partial^4 h}{\partial x^4}. \quad (1)$$

The second term in Eq. (1) amplifies perturbations to a flat step edge in the manner suggested. The last two terms in Eq. (1) are familiar from extensive studies of the effect of capillary smoothing on the morphology of step edges on vicinal surfaces.<sup>11,19</sup> The second derivative term models evaporation-condensation events where atoms detach from a step edge, migrate rapidly on the adjacent terrace, and reattach to the step elsewhere. The fourth derivative term models edge diffusion events where atoms migrate along the step



FIG. 1. (Color online) Atomic force microscope image from Ref. 12 of a SiC(0001) surface graphitized at  $T \sim 1600$  °C in an induction furnace with a background Si pressure  $P \sim 1 \times 10^{-5}$  torr. The field of view is 10  $\mu\text{m}$ . The steps descend from left to right.

edge itself. In Eq. (1),  $a$  is the SiC lattice constant,  $\sigma = a^3 \gamma / kT$  ( $\gamma$  is the SiC step stiffness),  $\Gamma = \nu \exp(-E_1/kT)$  is the mean rate at which atomic species detach from a straight SiC step ( $\nu$  is an attempt frequency) and  $D = a^2 \nu \exp(-E_2/kT)$  is the edge diffusion constant.

Kinetic theory relates the average step velocity to the difference between the flux of Si atoms subliming from the surface (as measured by the equilibrium vapor pressure of Si over SiC) and the background pressure  $P$  in the growth chamber:

$$V = \beta \frac{a^3}{\sqrt{2\pi m k_B T}} (P_{\text{eq}} - P). \quad (2)$$

In this expression,  $m$  is the mass of a Si atom,  $\log_{10} P_{\text{eq}}(\text{Pa}) = 12.74 - 2.66 \times 10^4 / T(^{\circ}\text{K})$ ,<sup>20</sup> and  $\beta$  is the evaporation coefficient.<sup>21</sup> We note that increasing  $P$  shifts  $T_G$  to higher temperature and no decomposition occurs if  $P$

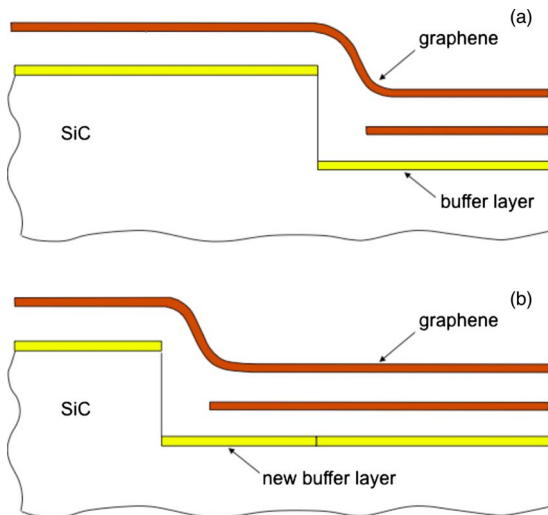


FIG. 2. (Color online) Graphene growth at a step on SiC(001): (a) initial state; (b) final state.

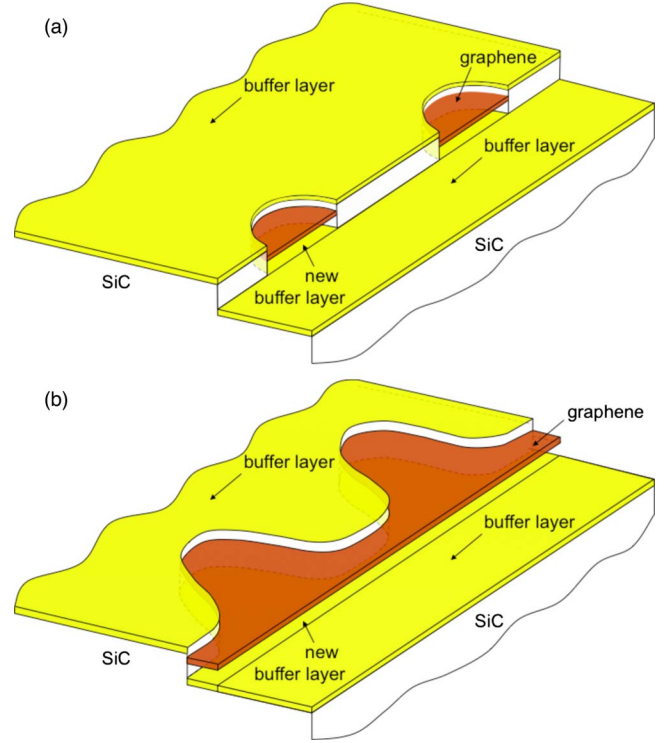


FIG. 3. (Color online) Onset of instability: (a) thermal decomposition of SiC starts at random points along the step edges; (b) a positive feedback mechanism promotes further decomposition and graphitization where it has already begun. The topmost complete graphene layer is not shown.

$> P_{\text{eq}}$ .<sup>22</sup> It is straightforward to perform a linear stability analysis of Eq. (1) assuming a solution of the form  $h(x, t) = -Vt + \epsilon(t) \sin(2\pi x/\lambda)$ . The perturbation amplitude  $\epsilon(t)$  growth (decays) exponentially when the wavelength  $\lambda$  is greater (less) than a critical wavelength. The most unstable (fastest growing) wavelength is

$$\lambda_m = \sqrt{\frac{8\pi^2 \sigma D}{aV - \sigma \Gamma}}. \quad (3)$$

The constants that enter  $\lambda_m$  that require special discussion are  $\gamma$ ,  $E_1$ ,  $E_2$ , and  $\beta$ , since none of these is truly known for SiC. For the step stiffness of a three-bilayer step, we chose  $\gamma = 1$  eV/Å, which is approximately three times the stiffness of steps on Si(111).<sup>19</sup> The detachment and surface diffusion barriers were chosen as  $E_1 = 5.6$  eV and  $E_2 = 5.0$  eV based on values for surface diffusion barriers for C atoms and Si atoms on several SiC surfaces given by Fissel.<sup>23</sup> The evaporation coefficient was fixed at  $\beta = 0.046$  to make the calculated growth rate equal the experimental growth rate associated with Fig. 1.

Figure 4 is a plot of  $\lambda_m$  as a function of growth temperature for several values of Si background pressure. There is no graphene growth when  $T < T_G$  and step edges are absolutely stable (no fingers) when  $T > T_S$ . Between  $T_G$  and  $T_S$ , there is a temperature window where the step edge is unstable. This window is largest for UHV growth and decreases as  $P$  increases. There is a critical pressure,  $P_S$ , above which

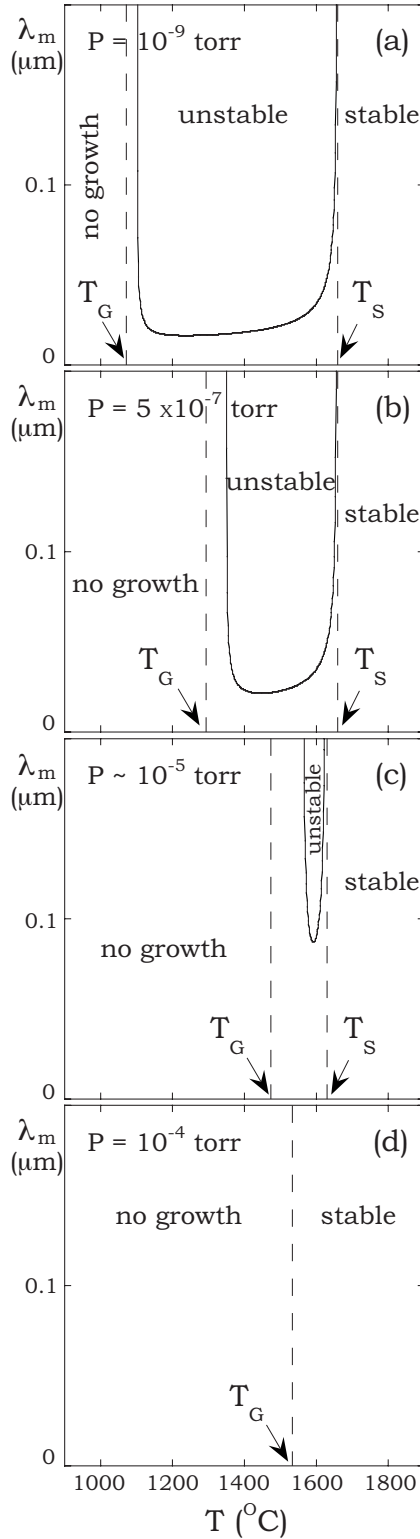


FIG. 4. Dependence of the fastest growing wavelength  $\lambda_m$  on the growth temperature  $T$  for several values of the background Si pressure  $P$ .

graphene growth occurs with no morphological instability of the SiC step edges. Below  $P_S$  and just above  $T_G$ , there is a narrow region of stable growth. All these features arise from the competition between the destabilizing curvature effect

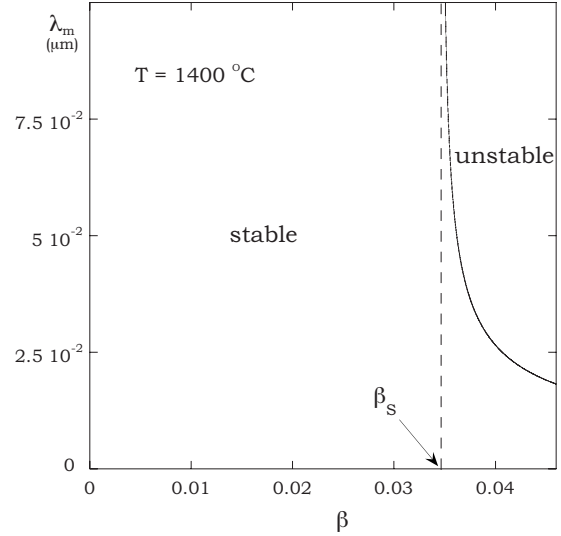


FIG. 5. Dependence of the fastest growing wavelength  $\lambda_m$  on the evaporation coefficient  $\beta$  for  $P=0$  and  $T=1400$  °C.

and the stabilizing effect of step edge evaporation/condensation and edge diffusion. The capillary forces of step smoothing always prevail when  $T > T_S$ . The narrow temperature range of edge stability just above  $T_G$  occurs because the destabilizing curvature term in Eq. (1) is proportional to  $V$ , which is very small near  $T_G$ . Otherwise, instability dominates and the scenario sketched in Fig. 3 occurs.

For the growth conditions stated in Fig. 1, Fig. 4(c) predicts a most unstable wavelength of  $\sim 0.1$   $\mu\text{m}$ . This agrees well with the separation between fingers in Fig. 1. Additional experiments where graphene was grown in a furnace with a higher value of background pressure produced only straight steps,<sup>24</sup> in qualitative agreement with Fig. 4(d). Figure 4(a) corresponds to an ultrahigh vacuum environment and so should be relevant to the graphene growth experiments reported in Ref. 16. At  $T \approx 1200$  °C, step edge fingers were observed with a mean separation of  $\lambda_m \sim 0.01$   $\mu\text{m}$ , which accords well with our theory. The fingers disappeared when the UHV experiments were repeated at  $T \sim 1350$  °C,<sup>25</sup> which agrees only semiquantitatively with Fig. 4(a). On the other hand, the value of the evaporation coefficient  $\beta$  in Eq. (2) depends on the kinetic pathway by which Si atoms escape into the vapor from the subsurface decomposition region. This pathway is unknown and doubtless depends on the sample preparation and defect structure, which we expect is not the same for the induction furnace experiment and the UHV experiment. A reduction of  $\beta$  by only a factor of two is sufficient to close the window in Fig. 4(a) enough to rationalize the UHV data.

We have mentioned that another process variable used in recent graphene growth experiments is the pressure of an inert gas intentionally introduced into the growth chamber.<sup>4,5</sup> The presence of such a gas tremendously improves the quality of the graphene produced epitaxially on SiC(0001). Presumably, the effect of the inert gas is to retard the escape of Si atoms from the decomposing crystal. The same thing happens in the present model if, as above, we reduce the value of the evaporation coefficient  $\beta$  in Eq. (2). Accordingly, Fig. 5

shows the dependence of the most unstable wavelength on  $\beta$  at  $T=1400^\circ\text{C}$  and  $P=0$ . There is a critical value,  $\beta_S$ , below which the theory predicts graphene growth without a step edge instability.

Finally, we propose a possible microscopic origin for the destabilizing  $-aV\partial^2 h/\partial x^2$  term in Eq. (1) based on the fact that the crystallization of free carbon atoms into new buffer layer material releases heat. This should transiently increase the local temperature and induce further decomposition. The result is a positive feedback mechanism that promotes further decomposition at points along the step where it has already begun.

In summary, we have shown that fingerlike step edges observed during the growth of epitaxial graphene by step flow decomposition of SiC(0001) can be understood from a competition between capillary smoothing and a curvature-driven mechanism for step edge roughening. A linear stability analysis of a step equation of motion that takes account of

all these effects predicts the separation between fingers as a function of the growth process variables: temperature, background Si pressure, and the influence of an inert gas in the growth chamber. The theory agrees semiquantitatively with growth experiments conducted in both a low-pressure induction furnace and under ultrahigh vacuum conditions. A local heating mechanism is proposed as the source of the instability.

The authors are grateful to M. Sprinkle and W. A. de Heer for permission to show the experimental data in Fig. 1. They also acknowledge helpful discussions with Phillip First, Edward Conrad, Miron Hupalo, Fan Ming, and Ming Ruan. The work of V.B. was supported by the Department of Energy under Grant No. DE-FG02-04-ER46170 and the MRSEC program of the National Science Foundation under Grant No. 0820382.

\*valery.borovnikov@physics.gatech.edu

†andrew.zangwill@physics.gatech.edu

<sup>1</sup>A. H. Castro Neto, F. Guinea, N. M. R. Peres, K. Novoselov, and A. K. Geim, *Rev. Mod. Phys.* **81**, 109 (2009).

<sup>2</sup>J. Hass, W. A. de Heer, and E. H. Conrad, *J. Phys.: Condens. Matter* **20**, 323202 (2008).

<sup>3</sup>J. Hass, R. Feng, T. Li, X. Li, Z. Song, W. A. de Heer, P. N. First, E. H. Conrad, C. A. Jeffrey, and C. Berger, *Appl. Phys. Lett.* **89**, 143106 (2006).

<sup>4</sup>C. Virojanadara, M. Syväjärvi, R. Yakimova, L. I. Johansson, A. A. Zakharov, and T. Balasubramanian, *Phys. Rev. B* **78**, 245403 (2008).

<sup>5</sup>K. V. Emtsev, A. Bostwick, K. Horn, J. Jobst, G. L. Kellogg, L. Ley, J. L. McChesney, T. Ohta, S. A. Reshanov, E. Rotenberg, A. K. Schmid, D. Waldmann, H. B. Weber, and T. Seyller, *Nature Mater.* **8**, 203 (2009).

<sup>6</sup>M. Orlita, C. Faugeras, P. Plochocka, P. Neugebauer, G. Martinez, D. K. Maude, A.-L. Barra, M. Sprinkle, C. Berger, W. A. de Heer, and M. Potemski, *Phys. Rev. Lett.* **101**, 267601 (2008).

<sup>7</sup>D. L. Miller, K. D. Kubista, G. M. Rutter, M. Ruan, W. de Heer, P. N. First, and J. A. Stroscio, *Science* **324**, 924 (2009).

<sup>8</sup>M. Fuhrer, *Nature (London)* **459**, 1037 (2009).

<sup>9</sup>P. Lauffer, K. V. Emtsev, R. Graupner, T. Seyller, L. Ley, S. A. Reshanov, and H. B. Weber, *Phys. Rev. B* **77**, 155426 (2008).

<sup>10</sup>G. S. Bales and A. Zangwill, *Phys. Rev. B* **41**, 5500 (1990).

<sup>11</sup>A. Pimpinelli and J. Villain, *Physics of Crystal Growth* (Cambridge University Press, New York, 1998).

<sup>12</sup>M. Sprinkle and W. A. de Heer (unpublished).

<sup>13</sup>S. Nie, C. D. Lee, R. M. Feenstra, Y. Ke, R. P. Devaty, W. J. Choyke, C. K. Inoki, T. S. Kuan, and G. Gu, *Surf. Sci.* **602**, 2936 (2008).

<sup>14</sup>V. Borovnikov and A. Zangwill, *Phys. Rev. B* **79**, 245413 (2009).

<sup>15</sup>T. Filleter, K. V. Emtsev, Th. Seyller, and R. Bennewitz, *Appl. Phys. Lett.* **93**, 133117 (2008).

<sup>16</sup>M. Hupalo, E. H. Conrad, and M. C. Tringides, *Phys. Rev. B* **80**, 041401(R) (2009).

<sup>17</sup>A. Mattausch and O. Pankratov, *Phys. Rev. Lett.* **99**, 076802 (2007).

<sup>18</sup>This may be contrasted with the vacancy diffusion mechanism proposed to explain step fingering during the thermal annealing of GaAs(0001). See C. W. Snyder, J. Sudijono, C.-H. Lam, M. D. Johnson, and B. G. Orr, *Phys. Rev. B* **50**, 18194 (1994).

<sup>19</sup>H.-C. Jeong and E. D. Williams, *Surf. Sci. Rep.* **34**, 171 (1999).

<sup>20</sup>S. K. Lilov, *Diamond Relat. Mater.* **4**, 1331 (1995).

<sup>21</sup>J. P. Hirth and G. M. Pound, *J. Phys. Chem.* **64**, 619 (1960).

<sup>22</sup>R. M. Tromp and J. B. Hannon, *Phys. Rev. Lett.* **102**, 106104 (2009).

<sup>23</sup>A. Fissel, *Phys. Rep.* **379**, 149 (2003).

<sup>24</sup>M. Sprinkle and W. A. de Heer (private communication).

<sup>25</sup>M. Hupalo (private communication).